Article published online: 2024-03-11



# Imaging in the Causes of Secondary Hypertension: Unveiling the Hidden Culprits

Gopinath Periaswamy[1] Navya Christopher[1] Venkatesh Kasi Arunachalam[1] V. Mangalakumar[2] Vishnu Prasad Pulappadi[1] Gowtham Sembagoundenvalasu Mahadevan[1] Sriman R.[1] Rupa R.[1] Pankaj Mehta[1] Mathew Cherian[1]

[1] Department of Radiology, Kovai Medical Center and Hospital, Coimbatore, Tamil Nadu, India
[2] Department of Nephrology, Kovai Medical Center and Hospital, Coimbatore, Tamil Nadu, India

**Address for correspondence** Venkatesh Kasi Arunachalam, DMRD, DNB, FRCR, MOI, Department of Radiology, Division of Abdominal & Transplant Imaging and Ablative Therapies, Kovai Medical Center and Hospital, Avanashi Road, Coimbatore, Tamil Nadu 641014, India (e-mail: drkasivenkatesh@yahoo.co.in; radvenki79@gmail.com).

Indographics 2024;3:246–254.

## Abstract

Secondary hypertension refers to the cases of hypertension having a specific underlying etiology. Secondary hypertension can be further divided to endocrine or nonendocrine causes. Radiologists must accurately identify the secondary causes of hypertension, as many of them can be treated, and treatment can result in improved symptoms or resolution of hypertension. Secondary hypertension requires a thorough imaging investigation using ultrasound, Doppler ultrasound, computed tomography angiography, magnetic resonance imaging, scintigraphy, and other imaging techniques to identify the underlying cause for optimal management.

**Keywords**

- secondary hypertension
- endocrinological causes
- nonendocrinological causes

## Introduction

Secondary hypertension accounts for about 10% of all cases of hypertension, which refers to the cases of hypertension having a specific underlying etiology.[1,2] Secondary hypertension can be further divided to endocrine or nonendocrine causes. An onset of hypertension in patients younger than 30 years, acute increase in blood pressure in a previously controlled hypertensive patient, or accelerated hypertension leading to end-organ damage are signs that indicate secondary hypertension.[3] Imaging plays a vital role in the evaluation of a hypertensive patient, in order to establish the diagnosis of most cases of secondary hypertension, and to assess its complications and burden on the heart and the great vessels. In this review, we describe the imaging appearances of common causes of secondary hypertension (►**Fig. 1**).

## Endocrinological Causes of Secondary Hypertension

Endocrinological factors account for around 3% of all secondary hypertension cases.[4] These are characterized by increased hormone output and, in most cases, are treatable. Hypertension may be the first clinical symptom of a variety of endocrine diseases. Endocrine hypertension is most common in children and young people under the age of 40, and it can be caused by diseases involving the adrenal glands, pituitary gland, or sympathetic and parasympathetic ganglia extending from the base of the skull to the pelvis.[5]

### Conn Syndrome

Primary hyperaldosteronism (or Conn syndrome) is the most prevalent cause of secondary hypertension and is defined as increased autonomous production of aldosterone without

**DOI** https://doi.org/10.1055/s-0044-1782596.
**ISSN** 2583-8229.



Thieme Medical and Scientific Publishers Pvt. Ltd., A-12, 2nd Floor, Sector 2, Noida-201301 UP, India

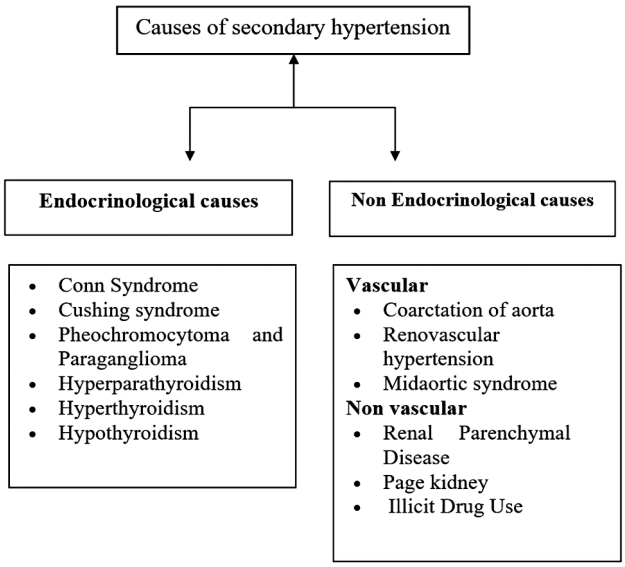


**Fig. 1** Common causes of secondary hypertension.

renin-angiotensin-aldosterone axis activation. It is frequently found in adrenal adenoma and hyperplasia. Adrenal cortical cancer, familial hyperaldosteronism syndrome, and ectopic aldosterone production (from an ovarian or renal source) are less prevalent causes.

Laboratory tests reveal a high aldosterone-to-renin ratio, hypokalemia, and a blood sodium level more than 140 mEq/L.[3] Adrenal adenoma imaging features in computed tomography (CT) include oval or round masses with a typical attenuation value of 10 Hounsfield unit (HU) or lower in non-enhanced CT, which has a high sensitivity and specificity of 79 and 96%, respectively. Other distinguishing characteristics of contrast-enhanced CT include absolute washout of 60% or more and relative washout of 40% or higher.[6,7] Absolute washout is defined as $[(HU_{1min} - HU_{15minD})/ (HU_{1min} - HU_{non})]$ x 100, and relative washout is defined as $[(HU_{1min} - HU_{15minD})/HU_{1min}]$ x 100, where $HU_{1min}$ is the attenuation value at 1 minute, $HU_{15minD}$ is the attenuation value at 15 minutes at delayed phase, and $HU_{non}$ is the attenuation value at nonenhanced CT. In circumstances when CT findings are ambiguous, chemical shift magnetic resonance (MR) can help distinguish adenoma from other lesions. Because the adenoma contains intracellular fat, the signal in out of phase imaging will be reduced (►**Fig. 2**). The diagnostic criteria for an adenoma are a drop in signal strength of more than 16.5%.[8]

## Cushing Syndrome

Despite the fact that Cushing syndrome is a rare cause of hypertension, hypertension affects 75 to 80% of Cushing syndrome patients.[9] This is caused by an overabundance of

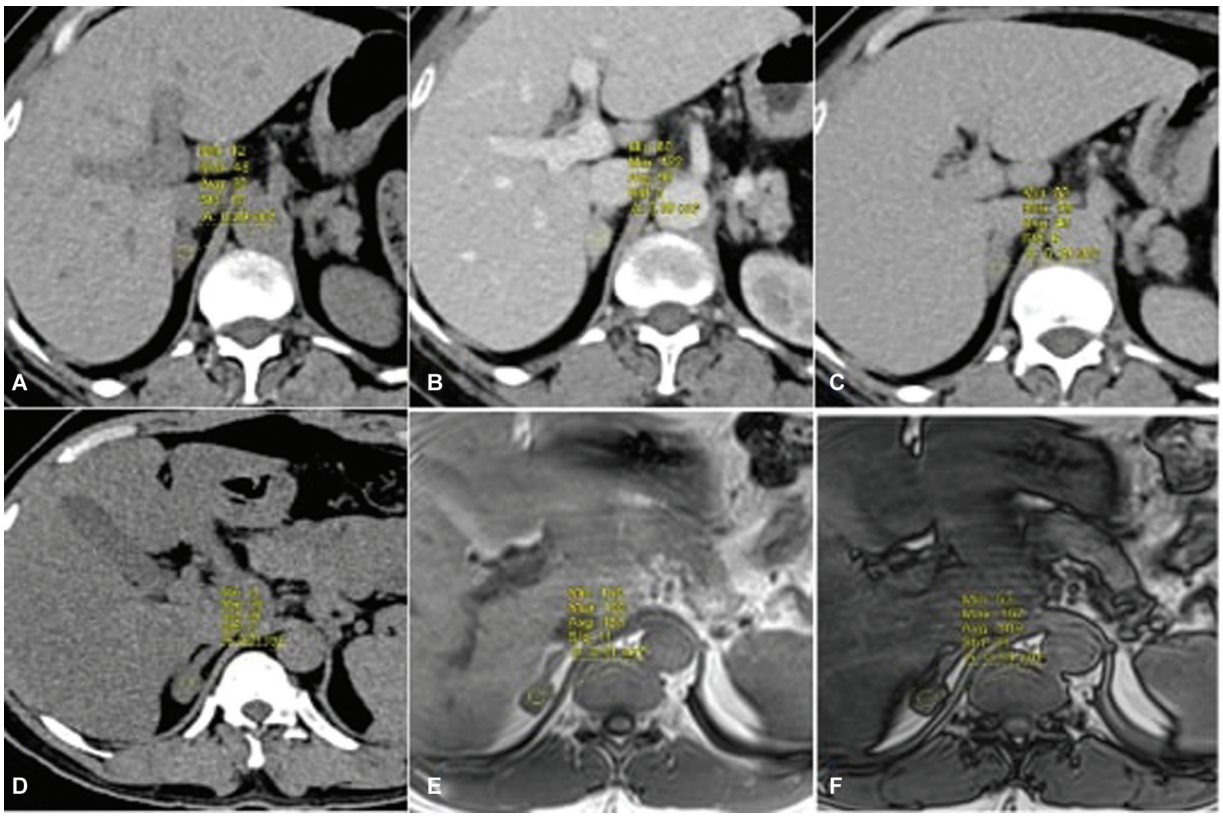


**Fig. 2** Adrenal adenoma. Axial noncontrast (**A**), venous phase (**B**), and 15 minutes delayed phase (**C**) images show a well-defined nodule in right adrenal gland with mean attenuation of 30 Hounsfield unit (HU) on noncontrast scan, with absolute contrast washout of 75%, suggestive of adrenal adenoma. (**D**) Axial noncontrast computed tomography image of another patient shows a well-defined nodule in right adrenal gland with mean attenuation of 29 HU. (**E, F**) Axial in-phase (**A**) and out-of-phase (**B**) magnetic resonance imagings of the same patient as in (**D**) show that there signal drop on out-of-phase image with signal intensity index of 33%, suggestive of adrenal adenoma.

 

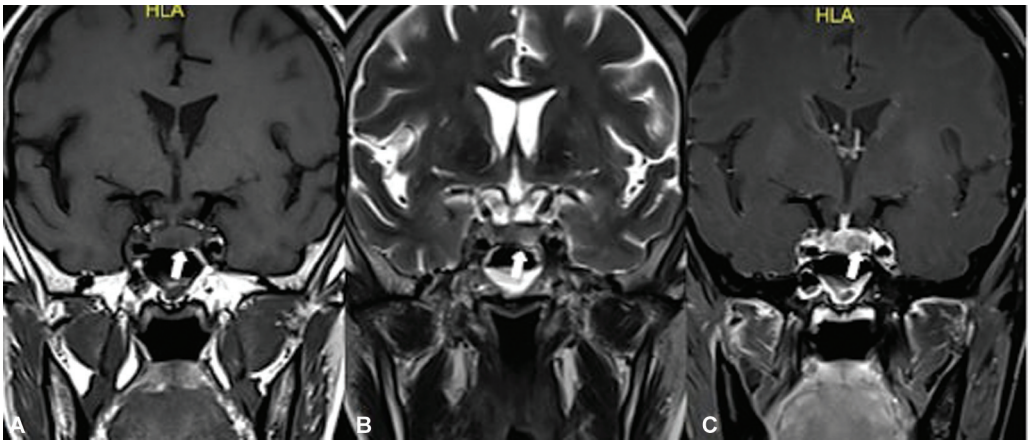


**Fig. 3** Pituitary microadenoma. Coronal T1-weighted (T1W) (**A**), T2W (**B**), and dynamic postcontrast T1W (**C**) images show a well-defined T1 hypointense and T2 hyperintense lesion in the left half of pituitary gland, with hypoenhancement compared to the pituitary gland parenchyma in the early arterial phase image (arrow), suggestive of pituitary microadenoma.

cortisol in the body and manifests clinically as moon facies, cervical fat pad, and pigmented striae. In dexamethasone suppression testing, laboratory results show hyperglycemia, hypokalemia, and a failure to suppress morning cortisol levels. Plasma adrenocorticotropic hormone (ACTH) levels aid in distinguishing between ACTH-dependent and ACTH-independent causes.

Cushing disease is caused by an excess of ACTH produced by a pituitary tumor (often a pituitary adenoma). Adrenal adenoma, paraneoplastic syndrome (most usually caused by small cell lung cancer), and adrenal cortical carcinoma, thymic carcinoid, medullary thyroid carcinoma, pancreatic neuroendocrine tumor, pheochromocytoma, and ovarian steroid cell tumor are all rare causes.[10]

Pituitary adenoma is a neuroendocrine tumor of the pituitary gland that is classified as microadenoma (less than 10 mm in size) (►**Fig. 3**) and macroadenoma (more than 10 mm in size) (►**Fig. 4**). Magnetic resonance imaging (MRI) is the preferred investigation for pituitary adenoma because it demonstrates asymmetric bulkiness of the pituitary gland and deviation of the infundibulum away from the tumor. Microadenoma identification requires a specific thin slice, dynamic contrast acquisition. In dynamic MRI, the microadenoma had delayed enhancement (90–120 seconds) compared to normal pituitary gland enhancement (60–80 seconds).[11] The nodule demonstrates varied enhancement on delayed imaging, resulting in a hypo, iso, or hyperenhancing nodule. In roughly half of the patients, the MRI may also be normal. Although CT is not advised routinely for pituitary adenoma because of its lesser sensitivity, it can be used when MRI is not an option. In cases when the MRI is normal, inferior petrosal sampling (IPS) could be utilized to confirm the presence of an ACTH-secreting microadenoma. IPS could be employed to lateralize the microadenoma as well.

## Pheochromocytoma and Paraganglioma

Pheochromocytoma (►**Fig. 5**) and paraganglioma (►**Fig. 6**) are uncommon tumors that account for fewer than 5% of all forms of hypertension. However, due to excessive catecholamine excretion, more than 90% of individuals with these lesions are hypertensive. Laboratory studies show higher 24-hour urine-fractionated metanephrine and catecholamine levels, as well as plasma metanephrine levels.[3]

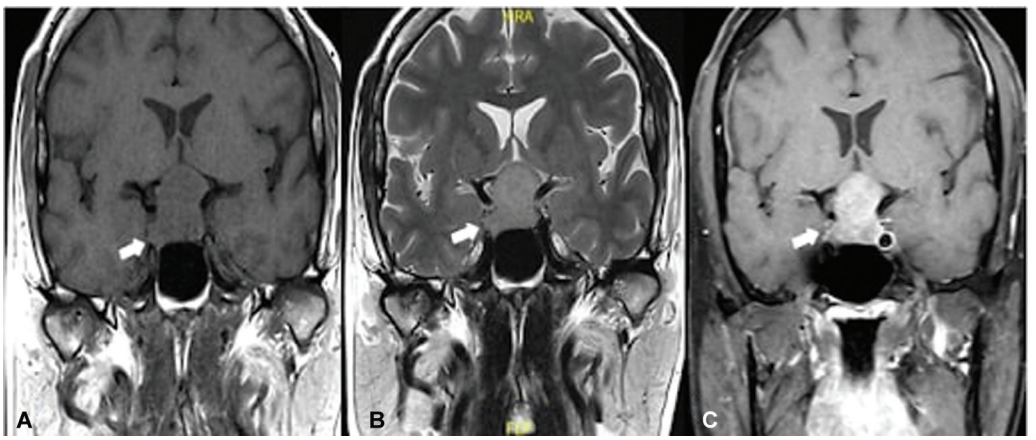


**Fig. 4** Pituitary macroadenoma. Coronal T1-weighted (T1W) (**A**), T2W (**B**), and postcontrast T1W (**C**) images show a well-defined T1 isointense, T2 hyperintense lesion occupying the sella and the suprasellar region showing homogeneous enhancement (arrow), suggestive of pituitary macroadenoma.

 

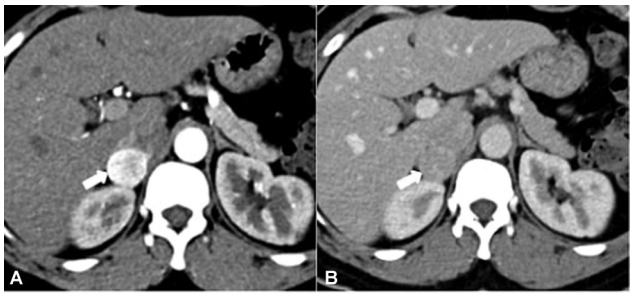


**Fig. 5** Pheochromocytoma. Axial arterial (**A**) and venous (**B**) phase images show a well-defined nodule in right adrenal gland with intense arterial phase enhancement and washout in the venous phase (arrow), suggestive of pheochromocytoma.

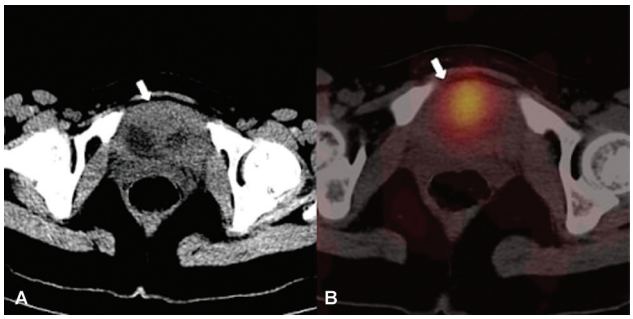


**Fig. 6** Paraganglioma. (**A**) Axial non contrast computed tomography image shows a polypoidal lesion arising from the anterior wall of the urinary bladder (arrow). (**B**) Meta-iodobenzylguanidine scan of the same patient shows intense tracer uptake within the lesion (arrow), suggestive of paraganglioma.

Pheochromocytoma develops from chromaffin cells in the adrenal glands, whereas paraganglioma develops from chromaffin cells outside the adrenal glands, such as sympathetic ganglia in the chest, abdomen, or pelvis, or parasympathetic ganglia at the base of the brain or along vagal or glossopharyngeal nerves.

Approximately 10 to 17% of pheochromocytomas and paragangliomas may be malignant. Most often sporadic, although 15 to 20% may be related to congenital diseases such as MEN-2A and 2B, neurofibromatosis I, tuberous sclerosis, von Hippel-Lindau disease, or familial pheochromocytoma–paraganglioma syndrome.[12,13] For imaging evaluations, CT is best for evaluating the chest, abdomen, and pelvis, and MRI is best for evaluating the skull base and neck and when metastases are suspected. Nuclear medicine tests, including iodine 123-MIBG scintigraphy, may be used if tumors cannot be seen on CT or MRI.

Pheochromocytomas and paragangliomas usually present as round or oval soft tissue masses that are 3 to 5 cm in size, but may be larger than 10 cm. Tumors may show areas of hemorrhage, calcifications, cystic change, necrosis, or fibrosis. Local spread to surrounding structures or distant metastases favor malignant tumors. On noncontrast CT, lesions measure more than 10 HU and in contrast enhanced CT lesions are significantly enhanced during the arterial phase or portal phase.[14] In some cases, the MRI appearance of a "light bulb–bright" mass with a cerebrospinal fluid-like signal may be seen on T2-weighted images. Most tumors appear isointense to muscle and hypointense to the liver on T1-weighted images. Because the lesions do not contain intracellular lipids, they do not produce the signal drop on out of phase contrast images as seen in adenomas. MRI contrast enhancement is noted similar to contrast-enhanced CT. Salt and pepper may appear in some paragangliomas due to flow voids.

## Hyperparathyroidism

Hypertension is seen in almost 50% of patients with primary hyperparathyroidism.[15] Laboratory screening tests reveal hypercalcemia and elevated serum parathyroid hormone. Parathyroid adenoma is the most common cause of hyperparathyroidism and the next common cause is parathyroid hyperplasia. Other less common causes include multiple parathyroid adenomas and parathyroid carcinoma.[16] Imaging investigations of choice are ultrasonography (USG) and technetium 99m–sestamibi scintigraphy, for preoperative localization of parathyroid, and show increased sensitivity when both examinations are done. A parathyroid adenoma (►**Fig. 7**) typically appears in USG as an oval hypoechoic nodule seen in juxta thyroidal location, mostly inferior or posterior to the thyroid gland with a

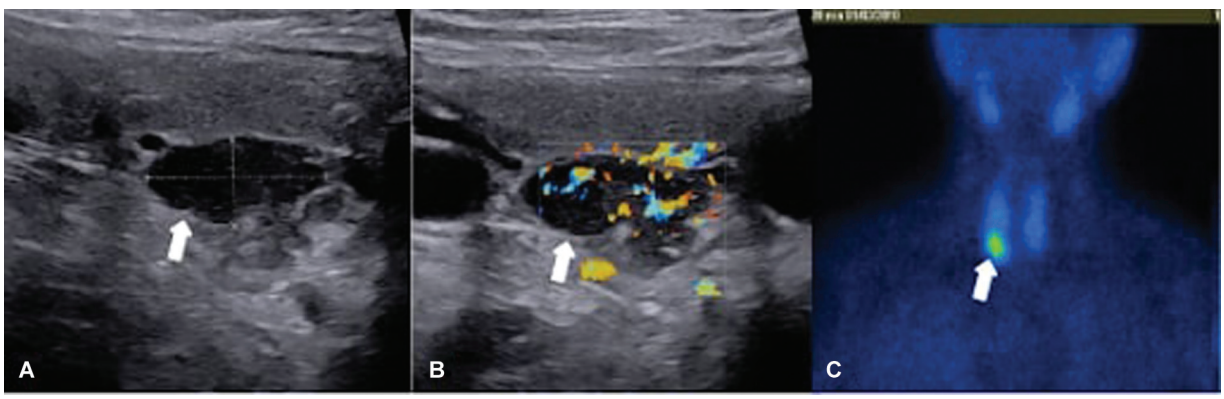


**Fig. 7** Parathyroid adenoma. B-mode (**A**) and color Doppler (**B**) ultrasonography images show a hypoechoic well-defined nodule adjoining the lower pole of right lobe of thyroid gland, with vascularity on Doppler (arrow). (**C**) Technetium Tc-99m sestamibi scan of the same patient shows intense tracer uptake within the nodule (arrow), suggesting of parathyroid adenoma.

 

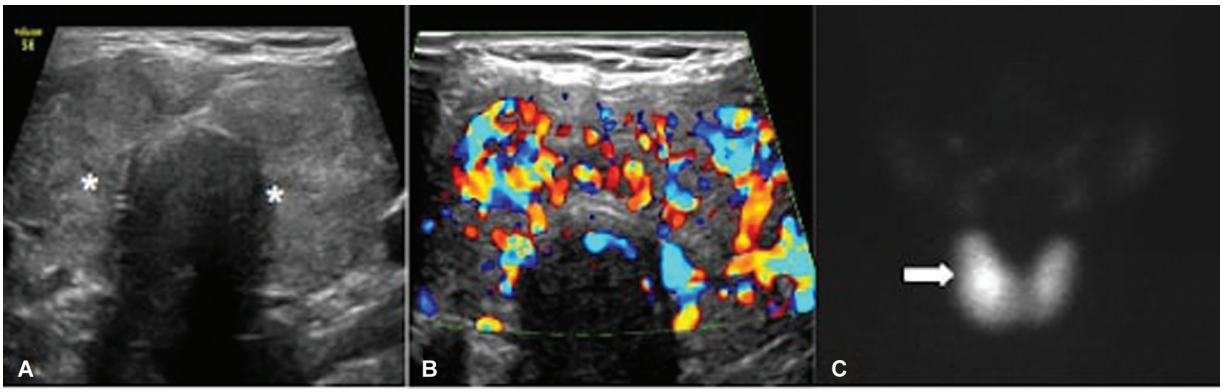


**Fig. 8** Grave's disease. B-mode (**A**) and color Doppler (**b**) ultrasonography images show diffusely enlarged thyroid gland (asterisks) with heterogeneous echogenicity and increased vascularity. (**C**) Technetium Tc-99m pertechnetate thyroid scan shows diffuse tracer uptake within the thyroid gland (arrow).

characteristic extrathyroidal feeding vessel seen in Doppler, entering the parathyroid from its pole showing arc or rim of vascularity.

Technetium 99m–sestamibi scintigraphy can be used to confirm nonectopic adenoma and localize ectopic adenomas. Most adenomas show avid tracer uptake and delayed washout compared to the thyroid tissue. Most adenomas have avid tracer uptake and delayed washout compared to thyroid tissue. CT and MRI may be performed if ectopic glands are suspected or if previous parathyroidectomy has failed.

## Hyperthyroidism

Approximately one-third of patients with hyperthyroidism have hypertension, which manifests primarily as increased systolic blood pressure due to increased heart rate, cardiac output, and decreased systemic vascular resistance. Clinical symptoms include increased appetite but weight loss, muscle weakness, heat intolerance, hyperhidrosis, and hyperadrenergic symptoms. The most common causes of hyperthyroidism are Graves' disease, toxic multinodular goiter, toxic adenoma, and thyroiditis.[9] Graves' disease (►**Fig. 8**) can also present as thyroid-related ophthalmopathy. Laboratory tests show a decrease in serum levels of thyroid-stimulating hormone. USG imaging features of Graves' disease include thyromegaly with heterogeneous echo texture and increased vascularity, showing a "thyroid inferno" pattern of vessels. CT and MRI are nonspecific, showing only a diffusely enlarged gland. Scintigraphy using iodine-131 and sodium pertechnetate shows increased activity in the enlarged gland. Toxic adenoma (►**Fig. 9**) can be single or multiple. These are benign monoclonal tumors that secrete excess thyroid hormone on their own. The probability of malignancy in these nodes is less than 1%. USG may show single or multiple nodules. On color Doppler, the nodules have both peripheral and intraparenchymal vascularity. In thyroid scintigraphy, a typical finding in toxic thyroid adenoma is a hot (hyperactive) nodule.

## Hypothyroidism

Hypothyroidism accounts for about 1% of cases of diastolic hypertension.[9] Laboratory tests show increased levels of thyroid-stimulating hormone. Clinical manifestations of hypothyroidism include lethargy, slurred speech, hoarse voice, cold intolerance, periorbital edema, constipation, enlarged tongue, brittle hair, and bradycardia. The most common cause is Hashimoto's thyroiditis. Others include

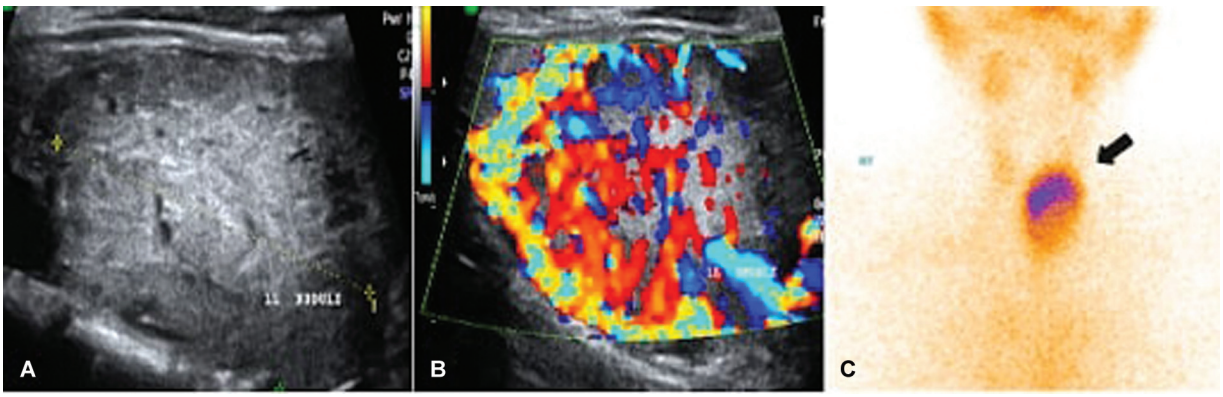


**Fig. 9** Toxic thyroid nodule. B-mode (**A**) and color Doppler (**B**) ultrasonography images of a patient with hyperthyroidism show an heteroechoic nodule with well-defined margins and intense vascularity in the left lobe of thyroid gland. (**C**) Technetium Tc-99m pertechnetate thyroid scan of the same patient shows focal tracer uptake within the nodule (arrow).

 

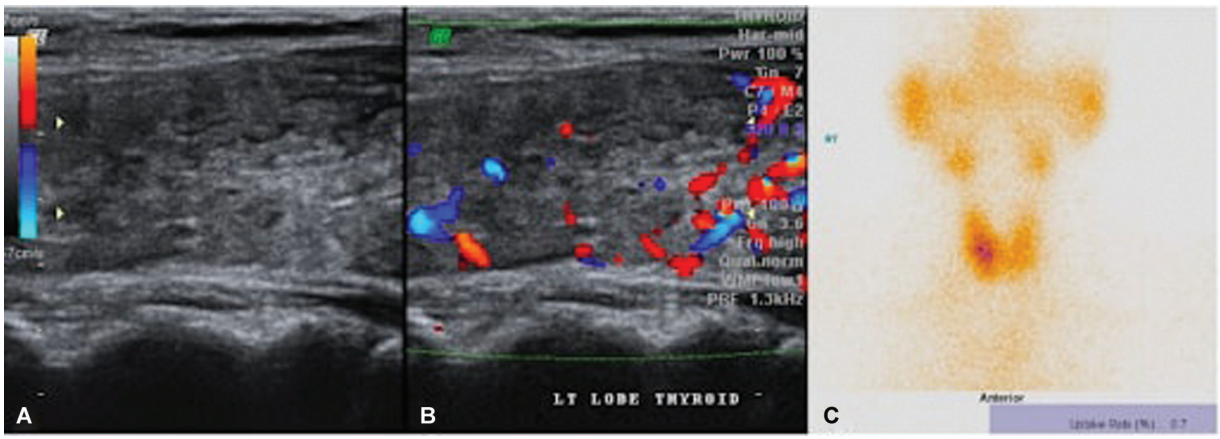


**Fig. 10** Hashimoto thyroiditis. B-mode (**A**) and color Doppler (**B**) ultrasonography images of a patient with Hashimoto thyroiditis show multiple small hypoechoic nodules with surrounding echogenic septations and reduced vascularity in the left lobe of thyroid gland. (**C**) Technetium Tc-99m pertechnetate thyroid scan of the same patient shows tracer decreased uptake in the left lobe of thyroid gland.

hyperthyroidism, thyroid surgery, radiation therapy, medications, thyroiditis, congenital hypothyroidism, pituitary disorders, pregnancy, and iodine deficiency. On USG, Hashimoto's thyroiditis (►**Fig. 10**) is seen as a diffusely enlarged thyroid gland with heterogeneous echoes and echogenic septa and variable vascularity. The presence of hypoechoic micronodules is very typical. Reactive cervical lymphadenopathy is common, especially at level VI.

## Nonendocrinological Causes of Secondary Hypertension

### Coarctation of Aorta

Coarctation of the aorta (►**Fig. 11**) refers to narrowing of the aorta adjacent to the origin of the left subclavian artery and ligamentum arteriosum, which can cause mechanical obstruction or renal ischemia leading to hypertension; and it is about 0.2% of hypertension cases.[17] Hypertension may persist or recur in patients even after coarctation repair. Clinical symptoms include claudication pain in the lower extremities, constant murmur over the back, or blood pressure in the thigh that is lower than in the upper arm.

CT angiography is the study of choice because it can provide high spatial resolution and accurately depict the location and severity of the coarctation. MR angiography can also accurately describe the location and severity of stenosis, which can be used for long-term follow-up, especially in children and young adults. Phase-contrast MR and four-dimensional flow techniques can be used to assess flow velocity and turbulence throughout the coarctation and to quantify collateral flow within the rest of the aorta.

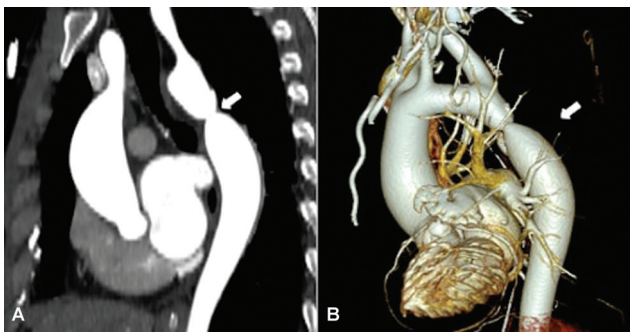


**Fig. 11** Coarctation of aorta. Sagittal oblique (**A**) and volume-rendered (**B**) images of computed tomography aortography show focal narrowing in the descending thoracic aorta, distal to left subclavian artery origin, suggestive of coarctation of aorta (arrow).

### Renovascular Hypertension

Renovascular disease accounts for about 1 to 2% of hypertension cases, with atherosclerotic disease or fibromuscular dysplasia being the most common causes. Less common causes are renal injury, dissection, arterial embolism, stent migration, and malignancy around the renal artery.[18] Laboratory tests show elevated serum creatinine, hypokalemia, and elevated serum creatinine with angiotensin-converting enzyme inhibitors or angiotensin II receptor blockers. USG and renal Doppler may be the first line of investigation that demonstrates increased peak systolic velocity (PSV) above 180 cm/s, increased renal–interlobar ratio, that is, $PSV_{renal\ artery\ (intrastenotic)}/PSV_{interlobar\ (distal)}$: greater than 5, increased renal–aortic ratio, that is, $PSV_{renal}/PSV_{aorta}$: more than 3.5, turbulent flow in a poststenotic area, pulsus parvus et tardus waveform due to stenosis, decreased (interlobar) renal arterial resistive index: less than 0.55 in severe stenosis, resistive index difference between kidneys more than 5%, intraparenchymal acceleration time more than 0.07 s and acceleration index: lower than 3 $m/s^2$.[19–22]

Recommended imaging is CT angiography (►**Fig. 12**) and MR angiography. Atherosclerotic disease usually results in focal narrowing of the proximal renal artery and, in fibromuscular dysplasia, narrowing and irregularities of the middle renal artery with characteristic string of beads appearance (►**Fig. 13**). CT angiography has a sensitivity and specificity of 94 and 99%, respectively, for diagnosing a stenosis of 50% or more, and MR angiography has a sensitivity and specificity of 90 and 86% for detecting a stenosis of 60% or more. Duplex USG has a sensitivity and specificity of 81 and 87% for the detection of 60% or greater stenosis.[23]

 


**Fig. 12** Atherosclerotic renal artery stenosis. Volume-rendered reconstruction (**A**) and axial oblique (**B**, **C**) images of arterial phase contrast-enhanced computed tomography show high-grade stenosis in bilateral renal artery ostia (arrows).

## Midaortic Syndrome

Midaortic syndrome (►**Fig. 14**) is a progressive narrowing of the abdominal aorta and its main branches. It is usually noted in children and young adults. The most common symptoms are high blood pressure, claudication pain, and kidney failure. Imaging findings include segmental narrowing of the thoracic or abdominal aorta, most often in the inter-renal segment, which includes the origin of the bilateral renal arteries. Dilated splanchnic arteries are seen with sparing of the iliac arteries and aortic bifurcation.[24] Color Doppler shows an increased PSV in narrow vessels (often around 230–480 cm/s) and a tardus-parvus pattern in the distal segments.[25]

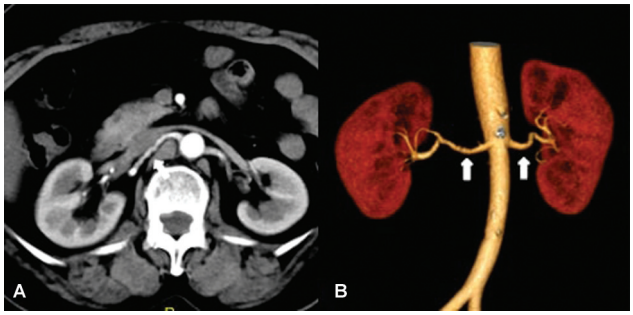


**Fig. 13** Fibromuscular dysplasia. Axial (**A**) and volume-rendered reconstruction (**B**) images of arterial phase contrast enhanced computed tomography show beaded appearance of bilateral main renal arteries (arrows), suggestive of fibromuscular dysplasia.

## Renal Parenchymal Disease

Another prominent cause of secondary hypertension is renal parenchymal disease, which is linked to over 75% of patients with acute glomerulonephritis and the majority of patients with autosomal dominant polycystic kidney disease (►**Fig. 15**).[26] Individuals who have diabetic nephropathy are also more likely to get hypertension. Increased intravascular volume or renin–angiotensin system activation causes hypertension. Serum creatinine levels are high, anemia, and hyper- or hypokalemia are seen in laboratory tests.[27] The renal parenchyma is shown as echogenic and thinned on USG, along with marginal abnormalities, papillary calcifications, decreased renal length, lack of cortico-medullary distinction, and poor visibility of the renal pyramids and renal sinus.

## Page Kidney

Page kidney (►**Fig. 16**) causes hypertension because subcapsular hematoma compresses renal parenchyma, triggering

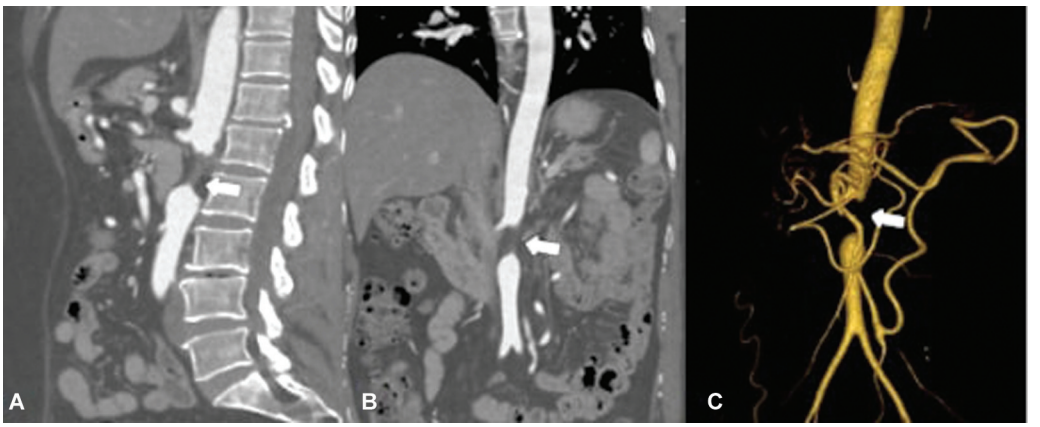


**Fig. 14** Middle aortic syndrome. Sagittal (**A**), coronal (**B**), and volume-rendered reconstruction (**C**) of computed tomography aortogram of a middle-aged lady show abrupt short segment narrowing of the contour with luminal occlusion of the infrarenal abdominal aorta (arrow). Adjacent segments of aorta are normal with no atherosclerotic changes.

 

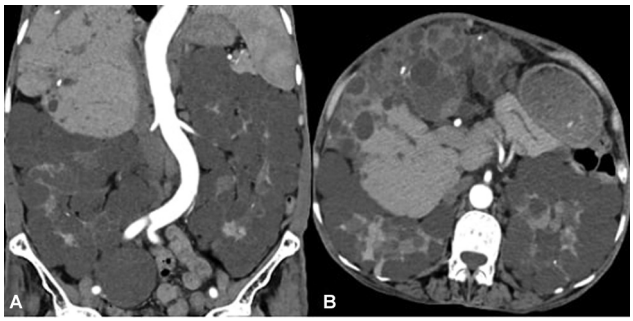


**Fig. 15** Autosomal dominant polycystic kidney disease. Coronal (**A**) and axial (**B**) contrast-enhanced computed tomography images show renal parenchyma replaced numerous cysts in both kidneys. Multiple simple cysts are seen in liver parenchyma as well.

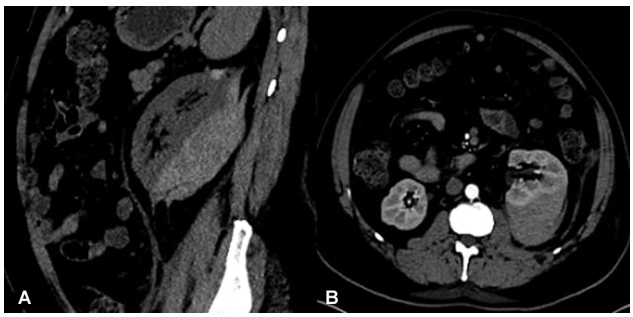


**Fig. 16** Page kidney. Sagittal (**A**) and axial (**B**) computed tomography images show subcapsular collection in the posterior aspect causing compression of the renal parenchyma.

the renin–angiotensin–aldosterone axis.[28] Subcapsular collections typically form in patients as a result of an initiating event, such as trauma or surgery. In certain instances, the cause may be the spontaneous burst of a cyst, aneurysm, or mass. Subcapsular collection with a mass effect in the underlying renal parenchyma might be seen on USG, CT, or MRI. Renal artery high resistive index can be found by Doppler USG. The collection may consist of seromas, urinomas, or hematomas.

### Illicit Drug Use

Elevated blood pressure can be caused by some pharmaceuticals, such as estrogen, herbal remedies, illegal substances like cocaine and amphetamines, steroids like prednisone and methylprednisolone, nonsteroidal anti-inflammatory drugs, lithium, tricyclic antidepressants, sympathomimetic decongestants, or diet pills. Acute hypertensive crises can also arise from cocaine use. Therefore, at the time of taking the first history, it is important to rule out the possibility of drug-induced hypertension.

## Conclusion

Secondary hypertension requires a thorough investigation to identify the underlying cause for optimal management. Advanced imaging modalities have revolutionized the diagnostic approach to secondary hypertension by providing noninvasive and highly accurate means to detect vascular, renal, and endocrine abnormalities that can contribute to elevated blood pressure. By utilizing USG, Doppler USG, CT angiography, MRI, scintigraphy, and other imaging techniques, clinicians can unravel the hidden culprits of secondary hypertension and offer targeted treatment strategies to improve patient outcomes. Early diagnosis and appropriate management of secondary hypertension not only control blood pressure but also help prevent further complications associated with underlying causes, leading to better overall health and quality of life for affected individuals.

**Funding**
None.

**Conflict of Interest**
None declared.

## References

1 Sinclair AM, Isles CG, Brown I, Cameron H, Murray GD, Robertson JW. Secondary hypertension in a blood pressure clinic. Arch Intern Med 1987;147(07):1289–1293
2 Anderson GH Jr, Blakeman N, Streeten DH. The effect of age on prevalence of secondary forms of hypertension in 4429 consecutively referred patients. J Hypertens 1994;12(05):609–615
3 Taler SJ. Initial treatment of hypertension. N Engl J Med 2018;378 (07):636–644
4 Sica DA. Endocrine causes of secondary hypertension. J Clin Hypertens (Greenwich) 2008;10(07):534–540
5 Gupta-Malhotra M, Banker A, Shete S, et al. Essential hypertension vs. secondary hypertension among children. Am J Hypertens 2015;28(01):73–80
6 Lattin GE Jr, Sturgill ED, Tujo CA, et al. From the radiologic pathology archives: Adrenal tumors and tumor-like conditions in the adult: radiologic-pathologic correlation. Radiographics 2014;34(03):805–829
7 Johnson PT, Horton KM, Fishman EK. Adrenal mass imaging with multidetector CT: pathologic conditions, pearls, and pitfalls. Radiographics 2009;29(05):1333–1351
8 Shetty AS, Sipe AL, Zulfiqar M, et al. In-phase and opposed-phase imaging: applications of chemical shift and magnetic susceptibility in the chest and abdomen. Radiographics 2019;39(01): 115–135
9 Young WF Jr, Calhoun DA, Lenders JW, Stowasser M, Textor SC. Screening for endocrine hypertension: an endocrine Society scientific statement. Endocr Rev 2017;38(02):103–122
10 Wagner-Bartak NA, Baiomy A, Habra MA, et al. Cushing syndrome: diagnostic workup and imaging features, with clinical and pathologic correlation. AJR Am J Roentgenol 2017;209(01): 19–32
11 Gardeur D. New Protocol for the MR Imaging of Pituitary Adenomas. Multiphase, Dynamic and Volumetric Imaging on MAGNETOM Skyra The Importance of StarVIBE and CAIPIRINHA Sequences. Siemens.Siemens MRI.
12 Plouin PF, Fitzgerald P, Rich T, et al. Metastatic pheochromocytoma and paraganglioma: focus on therapeutics. Horm Metab Res 2012;44(05):390–399
13 Bryant J, Farmer J, Kessler LJ, Townsend RR, Nathanson KL. Pheochromocytoma: the expanding genetic differential diagnosis. J Natl Cancer Inst 2003;95(16):1196–1204
14 Blake MA, Kalra MK, Maher MM, et al. Pheochromocytoma: an imaging chameleon. Radiographics 2004;24(Suppl 1):S87–S99
15 Das CJ, Baruah MP, Baruah UM. Radiological imaging in endocrine hypertension. Indian J Endocrinol Metab 2011;15(Suppl 4): S383–S388

 

16 Patel CN, Scarsbrook AF. Multimodality imaging in hyperparathyroidism. Postgrad Med J 2009;85(1009):597–605
17 Prisant LM, Mawulawde K, Kapoor D, Joe C. Coarctation of the aorta: a secondary cause of hypertension. J Clin Hypertens (Greenwich) 2004;6(06):347–350, 352
18 Herrmann SM, Textor SC. Current concepts in the treatment of renovascular hypertension. Am J Hypertens 2018;31(02):139–149
19 Li JC, Wang L, Jiang YX, et al. Evaluation of renal artery stenosis with velocity parameters of Doppler sonography. J Ultrasound Med 2006;25(06):735–742, quiz 743–744
20 House MK, Dowling RJ, King P, Gibson RN. Using Doppler sonography to reveal renal artery stenosis: an evaluation of optimal imaging parameters. AJR Am J Roentgenol 1999;173(03):761–765
21 Granata A, Fiorini F, Andrulli S, et al. Doppler ultrasound and renal artery stenosis: an overview. J Ultrasound 2009;12(04):133–143
22 Voiculescu A, Schmitz M, Plum J, et al. Duplex ultrasound and renin ratio predict treatment failure after revascularization for renal artery stenosis. Am J Hypertens 2006;19(07):756–763
23 Leung DA, Hoffmann U, Pfammatter T, et al. Magnetic resonance angiography versus duplex sonography for diagnosing renovascular disease. Hypertension 1999;33(02):726–731
24 Lewis VD III, Meranze SG, McLean GK, O'Neill JA Jr, Berkowitz HD, Burke DR. The midaortic syndrome: diagnosis and treatment. Radiology 1988;167(01):111–113
25 Yan L, Li H-Y, Ye X-J, Xu RQ, Chen XY. Doppler ultrasonographic and clinical features of middle aortic syndrome. J Clin Ultrasound 2019;47(01):22–26
26 Ihm CG. Hypertension in chronic glomerulonephritis. Electrolyte Blood Press 2015;13(02):41–45
27 Campese VM, Mitra N, Sandee D. Hypertension in renal parenchymal disease: why is it so resistant to treatment? Kidney Int 2006;69(06):967–973
28 Smyth A, Collins CS, Thorsteinsdottir B, et al. Page kidney: etiology, renal function outcomes and risk for future hypertension. J Clin Hypertens (Greenwich) 2012;14(04):216–221

 